Nonlinear Liquid Sloshing Analysis in a Cylindrical Container by Arbitrary Lagrangian-Eulerian Approach

Arbitrary Lagrangian-Eulerian 기법에 의한 원통형 유체저장구조물 내부유체의 비선형 슬러싱 해석

권 형 오* 조 경 환** 김 문 겸*** 임 윤 묵****
Kwon, Hyung-O Cho, Kyung-Hwan Kim, Moon-Kyum Lim, Yun-Mook

국문요약

유체자유수면의 동적거동을 합리적으로 예측하기 위해서는 비선형 특성을 보이는 자유수면의 동역학적 경계조건을 고려해야할 뿐만 아니라 시간에 따라 변화하는 자유수면의 위치변화에 따른 운동학적 경계조건을 고려하여야 한다. 이러한 문제는 대상구조물이 3차원이 될 경우 더욱 복잡해지므로 3차원 비선형 유체자유수면의 해석은 이론해의 도출이 어려우며 수치해석 방법을 이용하는 것이 효과적이다. 본 연구에서는 수치해석 안정성이 높고 3차원 문제에서도 하나의 변수로 유체거동을 모사할 수 있는 arbitrary Lagrangian-Eulerian approach 를 경계요소에 적용하여 효율적이며 안정적인 유체 대변형 해석기법을 개발하였다. 개발된 기법은 향후 자유수면의 비선형 효과를 고려한 유체-구조물 상호작용 해석에 효과적으로 적용할 수 있을 것으로 판단된다.

주요어 : 경계요소, arbitrary Lagrangian-Eulerian approach, 비선형 유체자유수면 거동

ABSTRACT

The solution to a liquid sloshing problem is challenge to the field of engineering. This is not only because the dynamic boundary condition at the free surface is nonlinear, but also because the position of the free surface varies with time in a manner not known a priori. Therefore, this nonlinear phenomenon, which is characterized by the oscillation of the unrestrained free surface of the fluid, is a difficult mathematical problem to solve numerically and analytically. In this study, three-dimensional boundary element method(BEM), which is based on the so-called an arbitrary Lagrangian-Eulerian(ALE) approach for the fluid flow problems with a free surface, was formulated to solve the behavior of the nonlinear free surface motion. An ALE-BEM has the advantage to track the free surface along any prescribed paths by using only one displacement variable, even for a three-dimensional problem. Also, some numerical examples were presented to demonstrate the validity and the applicability of the developed procedure.

Key words : boundary element, arbitrary Lagrangian-Eulerian approach, nonlinear free surface motion

1. Introduction

The motion of fluid with a free surface is one of the very interesting phenomena in many fields of engineering. A typical example of a free surface flow is sloshing in a container, which is subject to forced oscillation such as fuel sloshing of a liquid rocket propellant, oil oscillation in a large storage tank and water oscillation in a reservoir due to earthquake, and so forth. Many studies have been presented about sloshing problems with large amplitude. This phenomenon, called 'nonlinear sloshing' is analyzed mainly by numerical methods, which can be classified into three methods, i.e., the finite difference method, the finite element method and the boundary element method. Chen and Haroun[1] addressed the sloshing phenomenon in seismically-excited rectangular liquid storage tanks. The nonlinearity of both the kinematic and the dynamic conditions was considered. Because the location of the free surface is unknown, a numerical scheme was developed to transform a two dimensional uniform rectangular grid into boundary conforming curvilinear grid with prescribed arbitrary boundaries. Three-dimensional large amplitude sloshing in rectangular tanks has also been attempted. Nakayama and Washizu[2] proposed a nonlinear boundary element method by introducing an error correction term into the dynamic boundary condition, in order to suppress the numerical instability and dissipation. Okamoto and Kawahara[3] introduced a velocity correction method into the Lagrangian finite element formulation, and they justified their numerical method by comparing the numerical solutions with independent experimental results. Wu et al.[4]

* 연세대학교 사회환경시스템공학부, 박사과정
** 연세대학교 사회환경시스템공학부, 박사후연구원
*** 정회원 · 연세대학교 사회환경시스템공학부, 교수
(대표저자:applymkk@yonsei.ac.kr)
**** 정회원 · 연세대학교 사회환경시스템공학부, 부교수
본 논문에 대한 토의를 2005년 6월 30일까지 학회로 보내 주시면 그 결과를 게재하겠습니다. (논문접수일 : 2005. 3. 28 / 심사종료일 : 2005. 4. 15)

employed the open trapezoidal scheme for the stable time integration of nonlinear liquid sloshing in three-dimensional tank. Kasuga et al.[5], Ushijima[6] and Kim et al.[7] have performed numerical simulation of the three dimensional large amplitude liquid sloshing in a cylindrical containers subjected to horizontal and vertical excitation. Cho and Lee[8] introduce a velocity potential-based nonlinear finite element method for the accurate simulation of the large amplitude liquid sloshing in two-dimensional baffled tank subject to horizontal forced excitation.

The finite element method has been successfully applied to large free surface motion problems. Generally, it can be classified into three categories: namely, the Eulerian, Lagrangian and arbitrary Lagrangian-Eulerian (ALE) descriptions. The Eulerian approaches encounter many difficulties in trying to fit the free surface and often leads to inaccuracies. It is simple for the Lagrangian description to track a free surface, but usually it cannot cope easily with element distortions. Thus, an ALE viewpoint was introduced to the FEM to overcome the above shortcomings in both the Eulerian and the Lagrangian approaches. The ALE finite element method (FEM) has been applied with good results to large amplitude sloshing problem. However, this method requires a lot of computer storage because a liquid region must be subdivided into a large number of meshes, and such a tendency becomes more emphasized in three-dimensional problems.

The boundary element method (BEM) has gained recognition as a potent and computationally efficient method for the solution of boundary value problem in elastodynamics and potential problems. The attractive characteristic of BEM is that it only requires discretization of the surface of the problem domain, rather than the surface and the interior domain as required by FEM (Brebbia et al.[9]). Therefore, three-dimensional liquid region can be efficiently modeled by the boundary element method, which has the advantage of reducing the boundary surface in the global three-dimensional reference system to a two-dimensional system defined over the boundary surface.

In this study, three-dimensional boundary element method, which is based on the so-called an arbitrary Lagrangian-Eulerian approach for the fluid flow problems with a free surface, is formulated. An ALE-BEM has the advantage to track the free surface along any prescribed paths by using only one displacement variable, even for a three-dimensional problem. The introduction of the ALE description and treatment of nonlinear boundary conditions for a free surface in view of the ALE description are represented. Also, the solution procedure of an initial value problem for the evolutional system with free surface conditions is developed by the 4-th Runge-Kutta time integration scheme. Finally, some numerical examples are presented to demonstrate the validity and the applicability of the developed procedure.

2. Modelling of Liquid Region by ALE-BEM

2.1 Formulation of Liquid Region

The motion of a liquid in a three dimensional cylindrical tanks is shown in Figure 1, which is subjected to forced oscillation. Hydrodynamic pressure acts on the walls of a cylindrical tank, when the system is subjected to a seismic motion. For the simplicity of the problems, the liquid in the tank is assumed inviscid, incompressible, and the flow of the liquid is assumed to be irrotational and time harmonic. In view of these assumptions, the velocity potential are defined by

$$u_1 = \frac{\partial \phi(\mathbf{x},t)}{\partial x}, \quad u_2 = \frac{\partial \phi(\mathbf{x},t)}{\partial y}, \quad u_3 = \frac{\partial \phi(\mathbf{x},t)}{\partial z} \tag{1}$$

where, $\mathbf{x} = (x, y, z)$ is the position vector of the liquid and u_1, u_2, u_3 are the Eulerian velocity. The equation of motion for this liquid can be represented as follows.

$$\nabla^2 \phi(\mathbf{x},t) = 0 \tag{2}$$

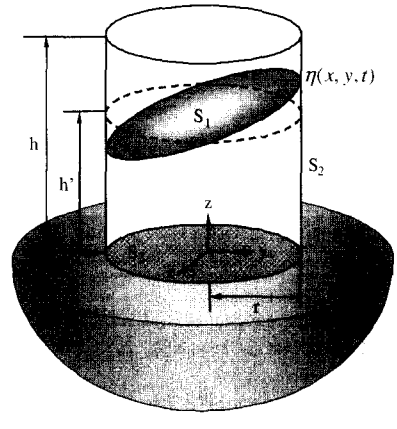

Figure 1 3-Dimensional Liquid Storage Tank and Coordinate System

Equation (2) is the Laplace equation and boundary integral equation derived from Lagrange-Green Identity can be written as follows

$$\phi(\xi,t)=\int_{\Gamma}\phi^{*}(\xi,\mathbf{x},t)\frac{\partial\phi(\xi,t)}{\partial\mathbf{n}}d\Gamma-\int_{\Gamma}\frac{\partial\phi^{*}(\xi,\mathbf{x},t)}{\partial\mathbf{n}}\phi(\xi,t)d\Gamma \tag{3}$$

where ξ is the source point and $\mathbf{x}$ is the receive point and $\phi^{*}(\xi,\mathbf{x},t)$ is the fundamental solution of Laplace equation or Green function. Green function, $\phi^{*}(\xi,\mathbf{x},t)$, satisfies that

$$\nabla^{2}\phi^{*}(\xi,\mathbf{x},t)+\Delta^{i}=0 \tag{4}$$

where Δ^{i} is the Dirac Delta function.

If the fundamental solution $\phi^{*}(\xi,\mathbf{x},t)$ and the traction $\partial\phi^{*}(\mathbf{x}^{i},\mathbf{x},t)/\partial\mathbf{n}$ apply to the Equation (3), we need to find out what happens when the point ξ is on Γ. The point, ξ, then becomes a boundary point and the resulting expression the specialization of Equation (3) for a point on Γ. Considering this singularity, we can get the boundary integral equation.

$$c(\xi,t)\phi(\xi,t)=\int_{\Gamma}\phi^{*}(\xi,\mathbf{x},t)\frac{\partial\phi(\xi,t)}{\partial\mathbf{n}}d\Gamma-\int_{\Gamma}\frac{\partial\phi^{*}(\xi,\mathbf{x},t)}{\partial\mathbf{n}}\phi(\xi,t)d\Gamma \tag{5}$$

Equation (5) for a boundary point is the boundary integral equation that will be solved numerically. To do so, the boundary surface is discretized into a series of elements over which the potential ϕ and the flux $\partial\phi/\partial\mathbf{n}$ are written in terms of their values at a series of nodal points. Writing the discretized form of equation (5) for every nodal point, a system of linear algebraic equations is obtained. The boundary surface in the global three-dimensional reference system can be reduced a two-dimensional system defined over the boundary surface. The complete boundary surface can be represented by boundary elements. The geometry of the surface and the associated distribution of unknowns are approximated within each element by interpolation from values at nodes that defined each element.

By those discretization procedure, Equation (5) can now be rewritten as matrix form in Equation (6) to give the global system of equations.

$$\mathbf{H}\boldsymbol{\varphi}=\mathbf{G}\frac{\partial\boldsymbol{\varphi}}{\partial\mathbf{n}} \tag{6}$$

where $\mathbf{H}$ and $\mathbf{G}$ have dimension $N\times N$ and $N\times 9NE$, respectively.

2.2 Nonlinear Boundary Conditions

2.2.1 Nonlinear Boundary Conditions of a Free Surface

There are two kinds of the boundary conditions to be prescribed. The first is the so-called free surface conditions on the free surface S_1. When fluid region with a free surface is subjected to an external excitation, the boundary conditions on the free surface S_1 are obtained by formulating the following two conditions (Stoker[10]).

(1) The pressure on the free surface must be equal to the atmospheric pressure (dynamic boundary condition).
(2) Liquid particles which are on the free surface remain on it during subsequent motion (kinematic boundary condition).

If the displacement of the free surface from its stationary position(sloshing height) is $\eta(x,y,t)$ as shown in Figure 1, the dynamic boundary condition is expressed by using Beroulli's pressure equation as

$$\frac{\partial\phi(\mathbf{x},t)}{\partial t}+\frac{P(\mathbf{x},t)}{\rho_{l}}+\frac{1}{2}\nabla\phi\nabla\phi+g\eta(x,y,t)=F(t) \tag{7}$$

where g is the gravitational acceleration, ρ_{l} is the liquid density and $P(\mathbf{x},t)$ is the hydrodynamic pressure. Assuming the atmospheric pressure to be zero, the dynamic and kinematic boundary conditions are expressed as follows.

$$\frac{\partial\phi(\mathbf{x},t)}{\partial t}+\frac{1}{2}\nabla\phi\nabla\phi+g\eta(x,y,t)=0 \quad ;\text{ at the free surface } (S_1) \tag{8}$$

$$\frac{D\mathbf{x}}{Dt}=\nabla\phi \quad ;\text{ at the free surface } (S_1) \tag{9}$$

The other is the boundary condition at the interface between liquid and tank wall (S_2). The boundary condition is that the normal component of the liquid velocity is equal to the tank wall velocity and expressed as

$\frac{\partial\phi(\mathbf{x},t)}{\partial\mathbf{n}} = v_n(t)$; at the interface between liquid and tank (S_2) (10a)

where $v_n(t)$ is the common velocity of the fluid and boundary surface in the normal to the surface. In the case of rigid walls, the boundary condition at the interface between liquid and tank wall is

$\frac{\partial\phi(\mathbf{x},t)}{\partial\mathbf{n}} = 0$; at the interface between liquid and tank (S_2) (10b)

The hydrodynamic pressure acting on wall can be derived by Equation (7).

$P(\mathbf{x},t) = -\rho_l \frac{\partial\phi(\mathbf{x},t)}{\partial t} - \rho_l \frac{1}{2}\nabla\phi\nabla\phi$; hydrodynamic pressure on S_2 (11)

2.2.2 Basic Theory of Arbitrary Lagrangian-Eulerian Description

Two classical viewpoints have been widely applied to describe the motion of a continuous medium. The first is the Eulerian, in which a spatial co-ordinate system independent of time that coincides with a laboratory reference frame is adopted to record the velocities or any other physical quantities of different fluid particles, which flow through the same co-ordinate point $\mathbf{X}(x,y,z)$ in the field at every moment. In the second, known as the Lagrangian, a material particle is always selected to be traced, and a description of its history of motion is needed. Usually, a fluid particle A is denoted by its orginal spatial co-ordinates (a,b,c); i.e.,

$\mathbf{A} = (a,b,c)$ (12)

The position change of the particle can be written as

$\mathbf{X} = \mathbf{X}^L(\mathbf{A},t)$ (13)

However, an ALE viewpoint (Hirt et al.[11]) may neither track a specific fluid particle nor observe its motion at a fixed co-ordinate point. It describes fluid movement at a computational node which is independent of the material motion and may be moved with an arbirary velocity in the laboratory system. A node point I is also denoted by its original spatial co-ordinates (i, j, k),

$\mathbf{I} = (i,j,k)$ (14)

and its chage of position by

$\mathbf{X} = \mathbf{X}^A(\mathbf{I},t)$ (15)

Let f be any physical quantity which is a continous function of the spatial variables and time but relative to the material particles. Such a physical quantity should be obtained simultaneously at a co-ordimate point where the fluid particle stays and simultaneously at a nodal point which contains the fluid particle. As is well known, a material time derivative is usually used in engineering analysis:

$\left.\frac{Df}{Dt}\right|_A = \frac{\partial f}{\partial t} + \frac{\partial f}{\partial \mathbf{X}} \cdot \left.\frac{\partial \mathbf{X}^L}{\partial t}\right|_X$ (16)

Similarly for a specified node, one has

$\left.\frac{Df}{Dt}\right|_I = \frac{\partial f}{\partial t} + \frac{\partial f}{\partial \mathbf{X}} \cdot \left.\frac{\partial \mathbf{X}^A}{\partial t}\right|_X$ (17)

where, $\partial f / \partial t$ is the local dervative and $\partial f / \partial \mathbf{X}$ is the gradient. $\partial \mathbf{X}^L / \partial t$ is the velocity of a fluid particle and $\partial \mathbf{X}^A / \partial t$ is the velocity of an ALE node.

In the general case, $Df / Dt|_I$ is not equal to $Df / Dt|_A$ except when $\partial \mathbf{X}^A / \partial t = \partial \mathbf{X}^L / \partial t$, which implies the Lagrangian description; and $Df / Dt|_I$ is not equal to $\partial f / \partial t$ except when $\partial \mathbf{X} / \partial t$, which implies the Eulerian description. The advantage of the ALE description is that the velocities of the mesh nodes can be choosen freely to control in part the nodal mevements by the computer so that element distortions can be avoided.

Consider now the introduction of the ALE viewpoint into the boundary element method. A curved surface equation for a moving boundary is expressed as

$F(\mathbf{X},t) = 0$ (18)

According to the kinematic boudnary condition that if $\mathbf{A}^*$ is a fluid particle on the free surface, it should remain on it during subsequent motion, one has

$F\left(\mathbf{X}^L(\mathbf{A}^*,t),t\right) = 0$ (19)

When the BEM is applied to a moving boudnary problem, it is necessary for a control node $\mathbf{I}^*$ to stay

on the boundary all the time. It follows from Equation (18) that one must have

$$F\left(\mathbf{X}^A(\mathbf{A}^*,t),t\right)=0 \tag{20}$$

Replacing f in both Equations (16) and (17) by F in both Equations (19) and (20) leads to

$$0=\left.\frac{DF}{Dt}\right|_{A^*}=\left.\frac{\partial F}{\partial t}+\frac{\partial F}{\partial \mathbf{X}}\cdot\mathbf{U}^L\right|_X \tag{21}$$

$$0=\left.\frac{DF}{Dt}\right|_{I^*}=\left.\frac{\partial F}{\partial t}+\frac{\partial F}{\partial \mathbf{X}}\cdot\mathbf{U}^A\right|_X \tag{22}$$

where $\mathbf{U}^L$ and $\mathbf{U}^A$ are the particle velocity and the node velocity at X, and $\partial F/\partial \mathbf{X}$ is the gradient of the boundary equation and possesses the same direction cosines as the normal $\mathbf{n}$. From Equations (21) and (22), an important conclusion is drawn:

$$\mathbf{n}\cdot\mathbf{U}^L=\mathbf{n}\cdot\mathbf{U}^A \tag{23}$$

This indicates that for an ALE-BEM node it is unnecessary to track a fluid particle as only the same velocity component in the normal direction of the surface is required. This enables one to command an element node to move along a presciribed path for the sake of preventing element distortions; for example, along a straight line, an inclined line, or even a curved line (Beskos[12]).

Here, Equation (23) is rewritten in the following form to replace the kinematic boundary condition, Eqaution (9).

$$\frac{\partial \eta}{\partial t}=|\nabla F|\cdot\frac{\partial \phi}{\partial \mathbf{n}} \quad \text{on} \quad z=\eta(x,y,t) \tag{24}$$

where, $|\nabla F|=\sqrt{\left(\frac{\partial \eta}{\partial x}\right)^2+\left(\frac{\partial \eta}{\partial y}\right)^2+1}$

3. Sloshing Analysis of Nonlinear Free Surface Flow

In this chapter, the numerical solution procedure for the large amplitude liquid sloshing in the rigid container subjected to horizontal forced excitation is developed using the boundary element method and the nonlinear boundary condition. The free surface configuration is tracked by the arbitrary Lagrangian-Eulerian approach and 4th order Runge-Kutta method is adopted as a direct time integration scheme.

3.1 Condensation of a Governing Equation

To analyses the free surface motion, the Equation (6) derived in previous chapter should be divided into a free surface region and a fluid-sturcure interface region. Therefore, boundary element Equation (6) can be presented following matrix form;

$$\begin{bmatrix}\mathbf{H}_{pp} & \mathbf{H}_{p\eta}\\ \mathbf{H}_{\eta p} & \mathbf{H}_{\eta\eta}\end{bmatrix}\begin{Bmatrix}\boldsymbol{\varphi}_p\\ \boldsymbol{\varphi}_\eta\end{Bmatrix}=\begin{bmatrix}\mathbf{G}_{pp} & \mathbf{G}_{p\eta}\\ \mathbf{G}_{\eta p} & \mathbf{G}_{\eta\eta}\end{bmatrix}\begin{Bmatrix}\boldsymbol{\varphi}_{p,\mathbf{n}}\\ \boldsymbol{\varphi}_{\eta,\mathbf{n}}\end{Bmatrix} \tag{25}$$

where subscript η and p denote the nodes for the free surface of liquid and the nodes on the fluid-structure interface, respectively.

Using matrix condensation procedure, Equation (6) can be condensed into the following three terms; $\boldsymbol{\varphi}_\eta$, $\boldsymbol{\varphi}_{\eta,n}$, $\boldsymbol{\varphi}_{p,n}$.

$$\hat{\mathbf{H}}_{\eta\eta}\boldsymbol{\varphi}_\eta=\hat{\mathbf{G}}_{\eta\eta}\boldsymbol{\varphi}_{\eta,n}+\hat{\mathbf{G}}_{\eta p}\boldsymbol{\varphi}_{p,n} \tag{26}$$

where, $\hat{\mathbf{H}}_{\eta\eta}=\mathbf{H}_{\eta\eta}-\mathbf{H}_{\eta p}\mathbf{H}_{pp}^{-1}\mathbf{H}_{p\eta}$, $\hat{\mathbf{G}}_{\eta\eta}=\mathbf{G}_{\eta\eta}-\mathbf{H}_{\eta p}\mathbf{H}_{pp}^{-1}\mathbf{G}_{p\eta}$, $\hat{\mathbf{G}}_{\eta p}=\mathbf{G}_{\eta p}-\mathbf{H}_{\eta p}\mathbf{H}_{pp}^{-1}\mathbf{G}_{pp}$

Consequently, the normal derivative of free surface potential vector is represented as

$$\boldsymbol{\varphi}_{\eta,n}=\hat{\mathbf{G}}_{\eta\eta}^{-1}\left(\hat{\mathbf{H}}_{\eta\eta}\boldsymbol{\varphi}_\eta-\hat{\mathbf{G}}_{\eta p}\boldsymbol{\varphi}_{p,n}\right) \tag{27}$$

Thus, the normal flux of the free surface can be determined by the free surface potential calculated using the nonlinear boundary conditions and the normal flux of the fluid-structure interface prescribed by the response of the structure.

3.2 Treatment of Nonlinear Boundary Conditions

To calculate the normal flux of the free surface using Equation (27) at each time step, the velocity potential of the free surface and the normal flux of the fluid-structure interface should be determined, as discussed in the previous Section 3.1. First, the normal flux of the fluid-structure interface can be determined by the response or the prescribed velocity of the structure in the previous time step using Equation (10). Second, in order to maintain stability in the numerical computations, the dynamic boun-

dary condition, Equation (8) should be treated carefully. The term $\partial\phi/\partial t$ is an Eulerian local derivative and must be converted into an ALE value by using Equation (22) before calculation.

$$\frac{\partial\phi}{\partial t} = \frac{D\phi}{Dt} - \left(\frac{\partial\phi}{\partial z}\right)\cdot\left(\frac{\partial\eta}{\partial t}\right) \tag{28}$$

Such a relationship brings the dynamic boundary condition into the form

$$\frac{D\phi}{Dt} + \frac{1}{2}\left\{(\nabla\phi)^2 - 2\cdot\left(\frac{\partial\phi}{\partial z}\right)\cdot\left(\frac{\partial\eta}{\partial t}\right)\right\} + (g + a_z)\eta + a_x x + a_y y = 0 \tag{29}$$

Using the rate of change of the velocity potential, Equation (29), the velocity potential of the free surface can be calculated by the direct time integration.

3.3 Solution Procedure

In order to solve the above nonlinear sloshing problem, the observation time interval is divided into a finite number of sub-intervals such that $t_n = k\cdot\Delta t$(k = 0,1,2,$\cdots$). Starting from the initial solutions ϕ^0 and η^0, the governing equation, Equation (2) defined in current flow domain, Γ^0 is successively solved to seek ϕ^k with the boundary condition, Equations (8)-(10). From which the condensed equation (27) is solved and the flux values $(\partial\phi/\partial\mathbf{n})^k$ can be obtained on a free surface. By using these potential gradients, fluid particle velocity filed $\mathbf{v}^k(u^k, v^k, w^k)$ and the sloshing velocity $\dot{\eta}$ are computed and the free surface tracking is performed. By the direct time integration of the free surface boundary conditions, Equations (24) and (29), ϕ^{k+1}, η^{k+1} and Γ^{k+1} are identified. In this paper, the following modified 4th-order Runge-Kutta scheme wherein the unknowns associated with the potential ϕ and $(\partial\phi/\partial\mathbf{n})$, but not the position of the free surface boundary, are updated in the intermediate steps.

3.4 Numerical Computation Techniques

In nearly all computations, the wave profile, after a sufficiently long time, developed a saw-toothed appearance, in which the computed positions of the particles lay alternatively above and below a smooth curve. The cause of the instability is that such high-wave number instabilities are non-physical and are closely related to the accuracy of the velocity calculations for the free-surface particles. Many researches showed that the rate of growth of the instability, per unit time, was independent of the number of time steps. Hence, it is not due simply to rounding errors. The growth may be partly physical, being similar to the growth of short gravity-waves by horizontal compressions of the crests of longer waves. In reality, these instabilities are partly damped by viscosity, which is neglected here.

The instability was effectively removed by the following procedure. A function $f(x)$ defined at equally spaced points x_j (j = 1,2,3), and in which alternate points lie on a smooth curve, can be locally approximated by two polynomials, say

$$h(x) = (a_0 + a_1 x + a_2 x^2 + \cdots + a_n x^n) + (-1)^j(b_0 + b_1 x + \cdots + b_{n-1}x^{n-1}) \tag{30}$$

The first bracket represents a smooth mean curve, the remainder a quantity that oscillates with period 2 in j. The coefficients $a_0, a_1, \cdots$ and $b_0, b_1, \cdots$ may be chosen uniquely so that $h(x) = f(x)$ exactly at (2n+1) consecutive points x_j, say (j-n) to (j+n) inclusive. Then, as a smoothed function, the even part can be taken.

$$\bar{h}(x) = a_0 + a_1 x + a_2 x^2 + \cdots + a_n x^n \tag{31}$$

In the case n=2, this leads to the 5-point smoothing formula as follows,

$$\overline{f_j} = \frac{1}{16}\left(-f_{j-2} + 4f_{j-1} + 10f_j + 4f_{j+1} - f_{j+2}\right) \tag{32}$$

The formula is applied for the calculated values of η and ϕ at every time-step. When the above 5 points cannot be taken at right or left end, the following modified formula is applied:

At right side, $$\overline{f_j} = \frac{1}{17}\left(-f_{j-2} + 4f_{j-1} + 10f_j + 4f_{j+1}\right) \tag{33}$$

At left side, $$\overline{f_j} = \frac{1}{17}\left(4f_{j-1} + 10f_j + 4f_{j+1} - f_{j+2}\right) \tag{34}$$

Next, the accuracy of numerical solutions gen-

erated by developed procedure is checked by estimating the volume of fluid occupied in container at each time step. If any change (i.e., increase or decrease) of the volume at some time step is found, the idea of adaptive refinement of boundary element mesh in numerical computation to avoid unreal change of liquid volume.

Lastly, all internal nodes are relocated such that the nodes located on the same vertical line should be in almost uniform spacing. In this manner, the free surface is tracked with the total liquid volume unchanged and the boundary element mesh is adapted to keep the mesh regularity fairly.

4. Verification of Liquid Sloshing Analysis

In this chapter, the numerical results of the small amplitude free oscillation were presented to verify the validity of the developed numerical algorithm. Then, in order to examine the applicability of the proposed solution procedure, the results of the horizontally forced oscillation were presented in the 3-D cylindrical container.

4.1 Small Amplitude Free Oscillation

A comparison of a number of data published in the literature with the present analysis is presented in this section. First, a free oscillation problem of fluids in a rigid cylindrical container, with has radius R and stationary state height H, as shown in Figure 2, was analyzed. The boundary of the fluid domain was divided into 72 elements and 242 nodes, and the free surface part was divided into 24 elements and 81 nodes, in Figure 2.

In numerical performance, the dimensions of the analysis models are r(radius)=0.5m, h'(height)=0.5m as the geometrical conditions of a container with the density of liquid equal to 1000kg/m^3. The time step size, Δt, was set to 5×10^{-3} sec throughout the numerical experiments. The initial profile of a free surface should be set up before the numerical performance on free oscillation. In this case, the following initial profile is η with i=1 and the small amplitude of A=0.1.

$$\eta(r,\theta)=\frac{A}{g}\left\{\sum_{i=1}^{\infty}\omega_i J_1\left(\frac{\varepsilon_i r}{R}\right)\cosh\left(\frac{\varepsilon_i H}{R}\right)\cos(\varepsilon_i t)\right\}\cos\theta \tag{35}$$

$$\omega_i^2=\frac{g}{R}\varepsilon_i\tanh\left(\frac{\varepsilon_i H}{R}\right) \tag{36}$$

Where, J_1 is the Bessel function of the first kind, ε_i is the i-th solution of $J_1'(\varepsilon R)=0$ and A is an arbitrary constant.

Figure 3 shows the curves $\eta(r,\theta)$ of the height of the free surface at two points ($r=R$, $\theta=0$ and $r=R$, $\theta=\pi$) against the time. The results were compared with those of the linear theory by Takayama[13] and the nonlinear theory by Kasuga et al.[5] Based on this figure, the results presented a good agreement with the linear theory.

4.2 Forced Horizontal Oscillation

To validate the present computational algorithm of the nonlinear analysis, the transient nonlinear problem of a cylindrical rigid container filled with water in 3-D was considered. The similar problem was solved by Kasuga et al.[5] and Ushijima[6] and the results are available in the literature. The container has the same dimensions as those in Section 4.1 and is subject to the sinusoidal forced horizontal acceleration of the type that is presented as

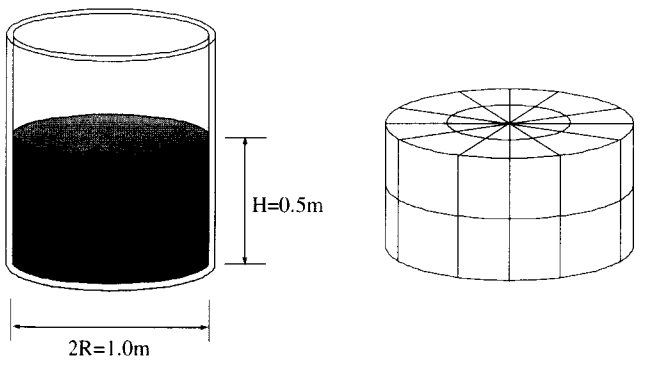

(a) Analysis Domain (b) Boundary Element Mesh

Figure 2 Analysis Domain and Boundary Element Mesh

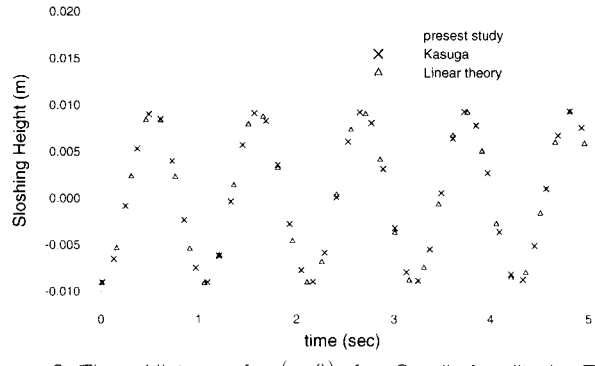

Figure 3 Time History of $\eta(r,\theta)$ for Small Amplitude Free Oscillation

$$a_x(t) = -X_0\omega^2 \sin\omega \cdot t \tag{37}$$

where, X_0 and w are the amplitude and the frequency of the forced horizontal displacement, respectively. In numerical performance, X_0=0.01m and w=5.85rad/s are adopted as parameters of the forced acceleration.

Figure 4 shows the boundary element mesh profile of the fluid domain, which is obtained using the Lagrangian approach, at different time steps before and after applying the smoothing technique, respectively. The severity of the mesh distortion may be observed after 2.65sec. These kinds of distortions lead to the numerical instability. To overcome this problem in the Lagrangian method, the smoothing (node repositioning) technique is adopted. After smoothing the mesh at every iteration of time integration, the numerical computations were advanced to obtain the required results. The boundary element mesh profile is shown in Figure 4. The advantage of the ALE description is that the velocities of the mesh nodes can be choosen freely to control, in part, the nodal mevements through the computer, so that element distortions can be avoided. Figure 5 shows the boundary element mesh profile using the ALE method without the mesh smoothing procedure. It was discovered that the mesh distortions were considerably reduced.

However, as shown in the dynamic boundary condition Equation (29), the material velocity obtained by the Lagrangian manner was used in the ALE method. Therefore, the smoothing techniques are necessary in order to avoid the unexpected numerical instability. Figure 6 shows the time history of the sloshing height at $r = R$, $\theta = 0$ and total volume change during analysis by ALE approach. Based on the results, it was determined that the mesh distortions can be avoided by the ALE method. However, to avoid the unexpected numerical instabilities, some techniques, such as the smoothing and the volume correction, must be considered.

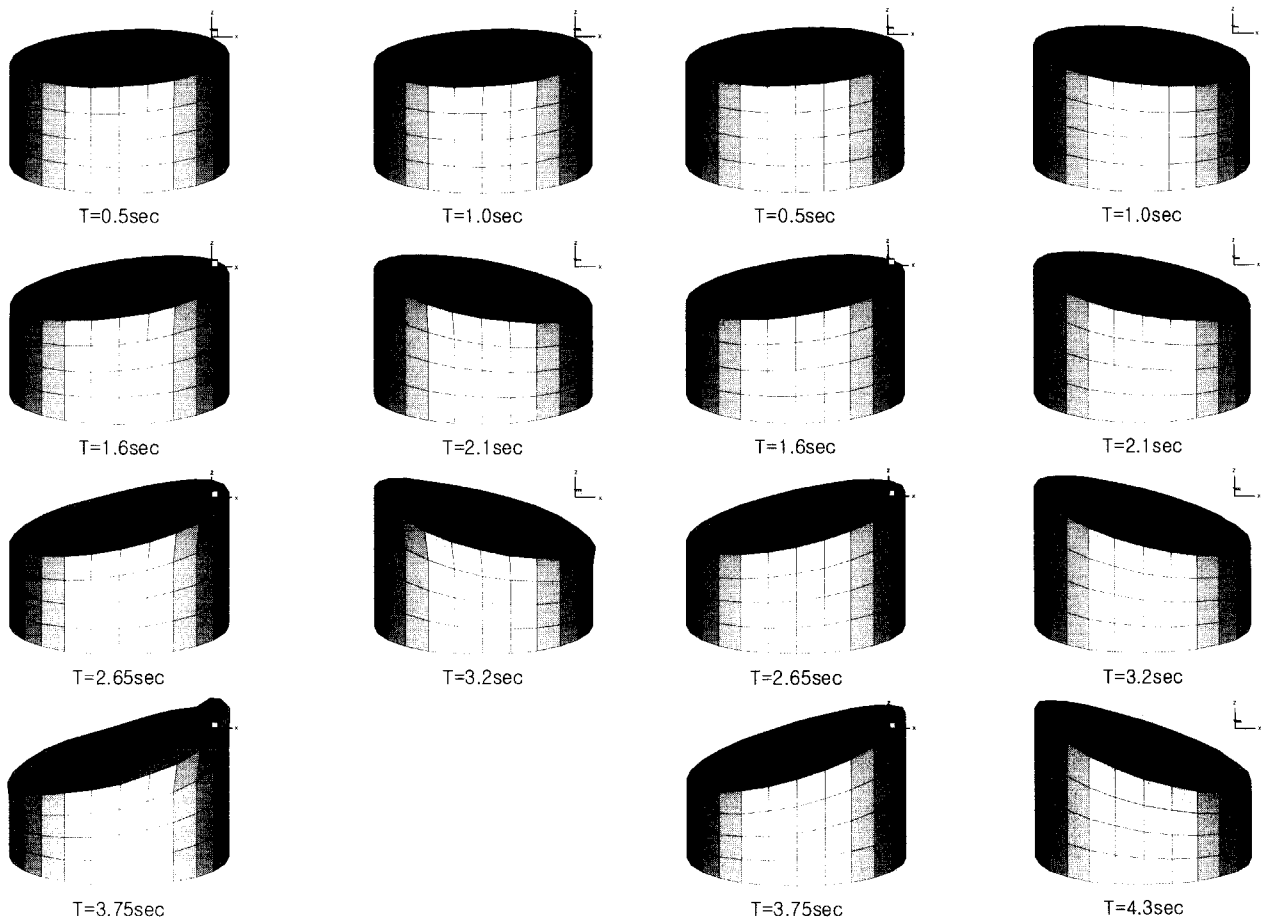

(a) Before Applying the Smoothing Technique (b) After Applying the Smoothing Technique

Figure 4 Mesh Profile by the Lagrangian Approach

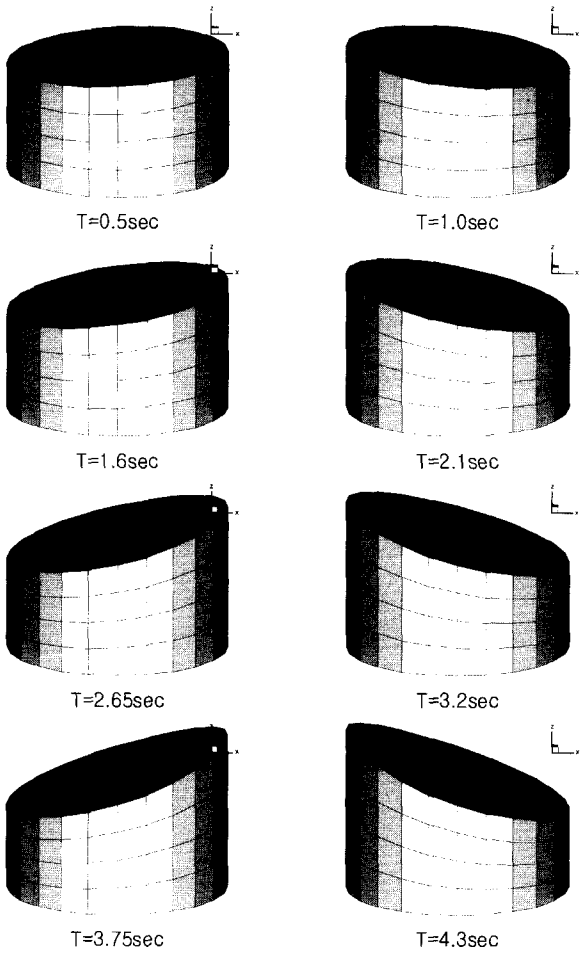

Figure 5 Mesh Profile by the ALE Approach

The results, shown in Figure 7 illustrate shows the time history of the sloshing height of the free surface at $r = R$ and $\theta = 0$ for both the linear and nonlinear free surface boundary conditions. The upward amplitude of sloshing becomes larger than the downward amplitude as time increases, indicating the typical non-linear characteristic of free surface sloshing. The results are quite similar to those reported by Ushijima[6], although the present amplitudes are slightly larger than their results, which were obtained considering the liquid viscosity.

Two significant terms of the dynamic boundary condition, varying in time at $r = R$ and $\theta = 0$ of the free surface, are shown in Figure 8. When the nonlinear sloshing height of the water wave rises above the linear sloshing height, the velocity squared terms $0.5\nabla\phi\nabla\phi$ becomes larger than $g \cdot \eta$. This is no longer a small quantity that can be ignored during the subsequent calculation. Thus, the nonlinear boundary conditions of the free surface must be considered in order to determine the exact sloshing height.

5. Conclusions

In this study, a numerical solution procedure has

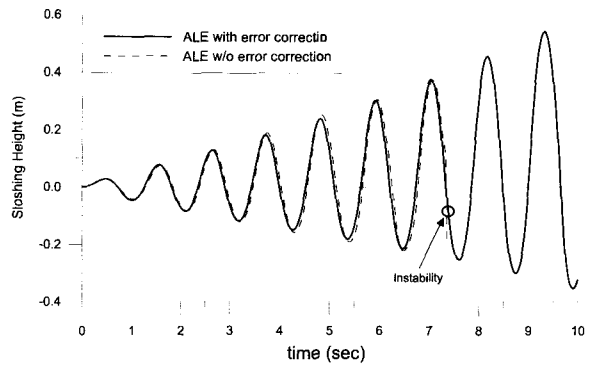

(a) Free Surface Elevation

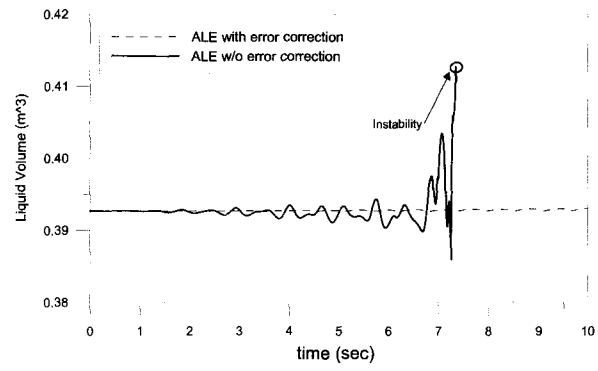

(b) Liquid Volume Conservation

Figure 6 Effects of Mesh Smoothing

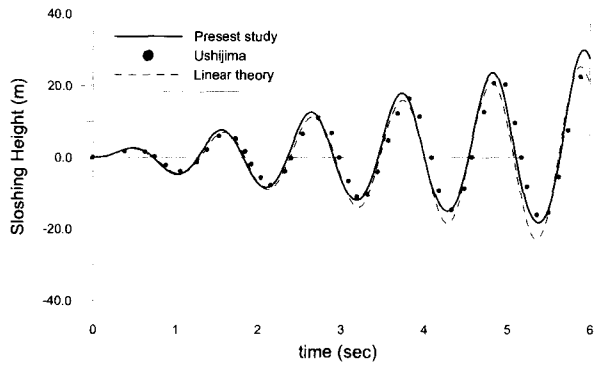

Figure 7 Time History of Sloshing Heights due to Forced Excitation

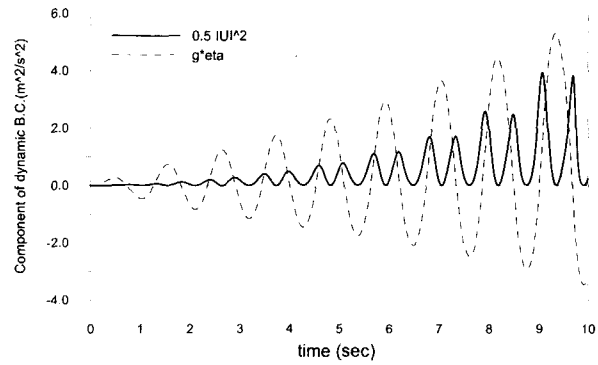

Figure 8 Time History of $0.5\nabla\phi\nabla\phi$ and $g \cdot \eta$ due to Forced Excitation

been developed in order to simulate large amplitude liquid motion in a cylindrical three-dimensional container. The procedure, which is based on the arbitrary Lagrangian-Eulerian description of a mathematical model of the problem, consists of the boundary element method and the solution algorithm with the 4-th order Runge-Kutta method. The ALE method reduces the numerical instabilities and the boundary element method requires discretization of the boundary surface rather than the volume. Additionally, to avoid numerical instabilities and accumulation error, numerical techniques, such as mesh smoothing and volume correction, are used. The developed method for the liquid region was validated through comparison of the analyses results with the published literature.

Through further study using developed algorithm, a numerical algorithm will be represented for the nonlinear coupled slosh dynamics of liquid storage tanks considering the flexibility of the container. From the results of this study, the free surface can be tracked by only one control displacement variable even though it was a three-dimensional problem. Thus, the entire equation of the nonlinear slosh dynamic problem can be coupled effectively based on the ALE-BEM. In order to construct the governing equation of the whole system, the finite elements of a structure and the boundary elements of a fluid region are coupled using the equilibrium and compatibility conditions, and the NFBC. Using these procedure, the dynamic behavior of a liquid storage tank considering fluid-structure interaction with nonlinear free surface boundary conditions can be studied more extensively.

References

1. Chen, W., Haroun, M.A. and Liu, F., "Large amplitude liquid sloshing in seismically excited tanks," *Earthquake Engineering and Structural Dynamics*, Vol.25, 1996, pp. 653-669.
2. Nakayama, T. and Washizu, K., "The boundary element method applied to the analysis of two-dimensional nonlinear sloshing problem," *International Journal for Numerical Methods in Engineering*, Vol.17, 1981, pp. 1631-1646.
3. Okamoto, T. and Kawahara, M., "Two-dimen sional sloshing analysis by the arbitrary Lagrangian-Eulerian finite element method," *Proceedings of JSCE, Structural Engineering/Earthquake Engineering*, Vol.8, No.4, 1992, pp.207-216.
4. Wu, G.X., Ma, Q.W. and Taylor, R.E., "Numerical simulation of sloshing waves in a 3D tank based on a finite element method," *Applied Oceans Research*, Vol. 20, 1998, pp.337-355.
5. Kasuga, L., Sugino, R. and Tosaka, N., "Sloshing motion in a cylindrical container by boundary element method," *Boundary Element Methods*, Eds. M. Tanata, Q. Du and T. Honma, Elsevier, 1993, pp.315-324.
6. Ushijima, S., "Three-dimensional arbitrary Lagrangian-Eulerian numerical prediction method for non-linear free surface oscillation," *International Journal for Numerical Methods in Fluids*, Vol.26, 1998, pp.605-623.
7. Kim, M.K., Lim, Y.M., Cho, K.H., Cho, S.Y. and Lee, S.M., "Three Dimensional Analysis of Large Sloshing Motion in a Fluid Container with Nonlinear Boundary Conditions," *Journal of KSCE*, Vol.22, No.5-A, 2002, pp.1093-1103.
8. Cho, J.R. and Lee, H.W., "Numerical Study on Liquid Sloshing in Baffled Tank by Nonlinear Finite Element Method," *Computer Methods in Applied Mechanics and Engineering*, Vol.193, 2004, pp.2581-2598.
9. Brebbia, C.A, Telles, J.C.F. and Wrobel, L.C., *Boundary Element Technique: Theory and Applications in Engineering*, Springer-Verlag, New York, 1984.
10. Stoker, J.J., *Water Waves*, Interscience Publishers, New York, 1954.
11. Hirt, C.W., Amsden, A.A. and Cook, J.L., "An arbitrary Lagrangian-Eulerian computing method for all flow speeds," *International Journal of Computational Physics*, Vol.14, 1974, pp.227-253.
12. Beskos, D.E., *Computational Methods in Mechanics 3: Boundary Element Methods in Mechanics*, Amsterdam, Elsevier, 1987, pp.400-401.
13. Takayama, T., "Theory of Transient Fluid Waves in a Vibrated Storage Tank," *Report of the Port & Harbour Research Institute*, Vol.15, No.2, 1976, pp.3-53.